Journal of Natural Gas Science and Engineering 49 (2018) 84–93

Contents lists available at ScienceDirect

Journal of Natural Gas Science and Engineering

journal homepage: www.elsevier.com/locate/jngse

Hydrogen/formic acid production from natural gas with zero carbon dioxide emissions

Jorge A. Pena Lopez, Ibubeleye Somiari, Vasilios I. Manousiouthakis*

Department of Chemical and Biomolecular Engineering, University of California, Los Angeles (UCLA), 5531 Boelter Hall, Los Angeles, CA 90095-1592, USA

ARTICLE INFO

Keywords:
Formic acid
Hydrogen
Natural gas
Energetic self-sufficiency
Reaction cluster
Heat and power integration

ABSTRACT

Presented in this work is a novel process flowsheet that co-produces hydrogen and formic acid from natural gas, without emitting any carbon dioxide. This is achieved by employing a reaction cluster that involves commercially available technologies, such as combustion, dry reforming, water-gas shift reaction, pressure-swing adsorption, and formic acid production via methyl formate hydrolysis. Thermodynamic and energetic self-sufficiency analysis imposes operating limits on the proposed process, within which a feasible flowsheet is developed. Heat and power integration analysis reveals that heat engine and heat pump subnetworks are sufficient to meet the flowsheet's energy requirements without violating energetic self-sufficiency constraints. Operating cost analysis reveals a revenue to cost ratio of 8.8, when the system's operating point is chosen to maximize hydrogen production.

1. Introduction

The use of oil derived gasoline as fuel for light vehicle based transportation has resulted over the years in two problematic issues: Poor air quality in large cities and increased emissions of carbon dioxide into the earth's atmosphere. The American Lung Association (American Lung Association, 2007) suggests that an estimated 136 million Americans – nearly 46% of the U.S. population – live in 251 counties with unhealthful levels of both ozone and particle pollution. According to the Earth System Research Laboratory (Pieter, 2017), the average concentration of CO_2 in the earth's atmosphere has increased from 316 ppm in 1960 to 346 ppm in 1985 and 406 ppm in 2017.

The use of hydrogen powered fuel cell vehicles has been proposed as an avenue for our society to address the aforementioned issues. Hydrogen is abundant in nature, although only in a combined state (e.g. water, hydrocarbons, carbohydrates) (Scholz, 1993). Its recovery from these natural resources requires the addition of energy (Spath and Mann, 2001). Hydrogen can be produced using a variety of energy resources (coal, oil, gas, biofuel, biomass, nuclear, solar, geothermal, wind, tidal power, wave power, hydro power, etc.) thus multiplying many-fold the availability of energy resources for transportation. Water is the only product of hydrogen's oxidation in an automotive fuel cell, and thus its use would completely address air quality issues in cities. Finally, hydrogen's production from renewable energy would not lead to carbon dioxide emissions to the atmosphere. The above, combined with the increased efficiency of hydrogen fuel cell vehicles over conventional gasoline vehicles, speak well as to the likelihood of adapting hydrogen as the next transportation energy carrier (Ramage and Agrawal, 2004). Although most renewable energy sources (solar, wind, geothermal, tidal power, wave power, hydro power) can be used to generate hydrogen using water electrolysis and thus generate no carbon dioxide emissions, such use would at the same time deprive our society of this electricity for its other needs. On the other hand, the prospect of carbon dioxide emissions has eliminated, in the mind of policy makers and environmentalists, the possibility of employing fossil fuels for the production of H_2, leading to the term “black hydrogen”. The thesis of this work is that hydrogen produced from a fossil fuel, such as natural gas, need not be “black”, but rather “green”, in both an environmental and economic sense.

In 2006, Posada & Manousiouthakis (Posada and Manousiouthakis, 2006) developed a process flowsheet that proposed producing hydrogen and dry ice to be sequestrated at the bottom of the ocean; and in our previous work (Pena Lopez and Manousiouthakis, 2011), we put forward the position that “hydrogen can be produced from fossil fuels

* Corresponding author.
E-mail addresses: jpenalopez@ucla.edu (J.A. Pena Lopez), isomiari@ucla.edu (I. Somiari), vasilios@ucla.edu (V.I. Manousiouthakis).

https://doi.org/10.1016/j.jngse.2017.11.003
Received 26 June 2017; Received in revised form 5 September 2017; Accepted 5 November 2017
Available online 07 November 2017

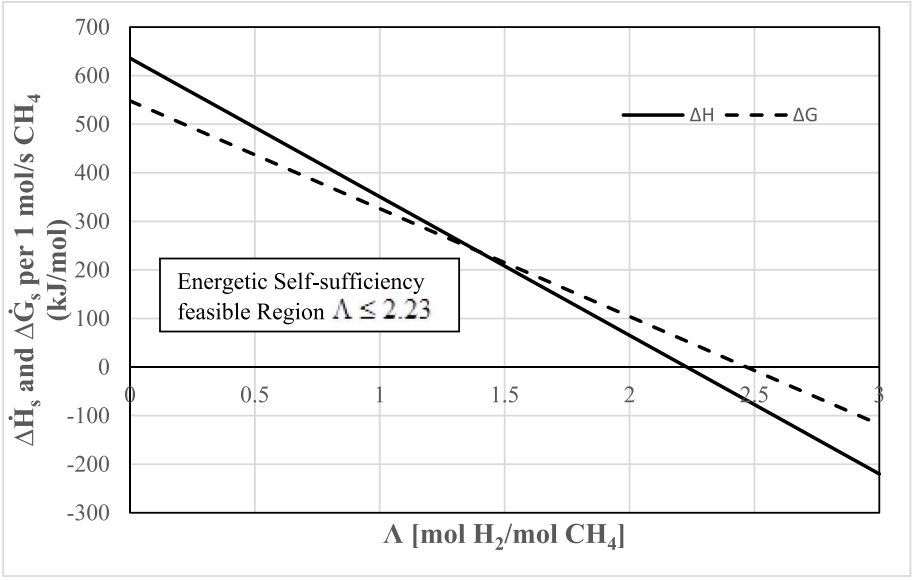

Fig. 1. Energetic Self-Sufficiency necessary conditions for overall reaction (3) using equations of (4).

without generation of carbon dioxide emissions". This was done by generating a process flowsheet co-producing hydrogen and formic acid, through a combination of steam methane reforming, combustion and formic acid production from carbon dioxide and hydrogen.

In this work, we build upon (Pena Lopez and Manousiouthakis, 2011) by proposing the co-production of hydrogen and formic acid with the use of commercially established technologies: dry reforming, combustion, water-gas shift and formic acid from methyl formate hydrolysis. The reactions at the heart of these technologies constitute a reaction cluster, whose realization is a novel process flowsheet with commercially proven subsystems. Heat and power integration techniques, such as was utilized in (Posada and Manousiouthakis, 2005), are then used to quantify the energy demands/production of this flowsheet, and to identify how heat engines and heat pumps can yield an energetically self-sufficient process, as defined in (Pena Lopez and Manousiouthakis, 2011), where no external heat or power is needed to meet the process energy needs.

The valuable carbon-containing product featured in this work is formic acid, which "absorbs" a molecule of carbon dioxide per molecule of hydrogen. Formic acid is a product with a global production of 640,000 metric tons/year. Its primary uses are leather treatment, preservative for silage, additive for rubber production, and as a thawing agent for icy surfaces. Finland is the world's leader in formic acid production, as represented by BASF and Kemira-Leonard. The commercial production of formic acid is typically carried out through hydrolysis of methyl formate followed by liquid-liquid extraction to purify the formic acid produced.

2. Energetic self-sufficiency and process reaction cluster

A process is energetically self-sufficient, iff its operation does not require external heat and power input (Pena Lopez and Manousiouthakis, 2011). Based on the principles of thermodynamics, the energetic self-sufficiency limits of a process flowsheet can be determined by carrying out energy and entropy balances as defined in Ref. (Pena Lopez and Manousiouthakis, 2011). An open well delimited system, that can potentially release heat $\dot{Q}_0 \leq 0$ to the environment at the environmental temperature T_0, is said to be energetically self-sufficient when the inequalities listed below are satisfied.

$$\left\{\begin{array}{l} \sum_{i\in S_I}\dot{m}_i - \sum_{i\in S_O}\dot{m}_i = 0 \\ \sum_{i\in S_I}\sum_{j\in S_C} v_{j,k}\frac{x_{i,j}}{M_j}\dot{m}_i - \sum_{i\in S_O}\sum_{j\in S_C} v_{j,k}\frac{x_{i,j}}{M_j}\dot{m}_i = 0 \qquad \forall\, k \in S_E \\ \dot{Q}_0 = T_0\cdot\left(\sum_{i\in S_O} S_i\dot{m}_i - \sum_{i\in S_I} S_i\dot{m}_i\right) - T_0\cdot\dot{S}_G \leq 0, \quad \dot{S}_G \geq 0 \\ \sum_{j\in S_W}\dot{W}_{s,j} = T_0\cdot\dot{S}_G - \left(\sum_{i\in S_I}(H_i - T_0\cdot S_i)\dot{m}_i - \sum_{i\in S_O}(H_i - T_0\cdot S_i)\dot{m}_i\right) \leq 0 \end{array}\right\} \tag{1}$$

A set of necessary conditions for energetic self-sufficiency originating from (1) is:

$$\left\{\begin{array}{l} \sum_{i\in S_I}\dot{m}_i - \sum_{i\in S_O}\dot{m}_i = 0 \\ \sum_{i\in S_I}\sum_{j\in S_C} v_{j,k}\frac{x_{i,j}}{M_j}\dot{m}_i - \sum_{i\in S_O}\sum_{j\in S_C} v_{j,k}\frac{x_{i,j}}{M_j}\dot{m}_i = 0 \qquad \forall\, k \in S_E \\ \sum_{i\in S_I} H_i\dot{m}_i - \sum_{i\in S_O} H_i\dot{m}_i \geq 0 \\ \sum_{i\in S_I}(H_i - T_0\cdot S_i)\dot{m}_i - \sum_{i\in S_O}(H_i - T_0\cdot S_i)\dot{m}_i \geq 0 \end{array}\right\} \tag{2}$$

If the inlets and outlets of a process are at the environmental temperature T_0, i.e. $T_i = T_0 \quad \forall\, i \in S_I \cup S_O$, then $H_i - T_0\cdot S_i = G_i$, if H_i, S_i, and G_i are respectively the system's specific enthalpy, entropy, and Gibbs free energy at $T_0 = 298.15\,K$. The concept of energetic self-sufficiency can now be applied to the proposed formic acid and hydrogen co-production process. The overall production of formic acid from natural gas can be represented by the following overall reaction:

$$CH_4 + \left(\frac{3-\Lambda}{2}\right)O_2 + (\Lambda - 1)\,H_2O \rightarrow HCOOH + (\Lambda)H_2 \tag{3}$$

This overall reaction (3) is parameterized by Λ, whose range is defined above by the requirement that oxygen should be consumed ($\Lambda \leq 3$), and below by the requirement that hydrogen should be produced ($\Lambda \geq 0$). For small values of Λ (i.e. $0 \leq \Lambda \leq 1$), this overall reaction consumes significant amounts of oxygen, produces small amounts of hydrogen, produces water, and generates significant amounts of energy. For larger values of Λ (i.e. $1 \leq \Lambda \leq 3$), this overall reaction consumes smaller amounts of oxygen, produces larger amounts of hydrogen, consumes water, and either generates smaller amounts of energy, or even becomes an energy consumer.

$$\left(\frac{3-\Lambda}{4}\right)\left[CH_4^{(g)} + 2O_2^{(g)} \rightarrow CO_2^{(g)} + 2H_2O^{(g)}\right] \quad (5)$$

$$\left(\frac{\Lambda+1}{4}\right)\left[CH_4^{(g)} + CO_2^{(g)} \rightarrow 2CO^{(g)} + 2H_2^{(g)}\right] \quad (6)$$

$$\left(\frac{\Lambda-1}{2}\right)\left[CO^{(g)} + H_2O^{(g)} \rightarrow CO_2^{(g)} + H_2^{(g)}\right] \quad (7)$$

$$CO^{(g)} + CH_3OH^{(l)} \rightarrow HCOOCH_3^{(l)} \quad (8)$$

$$HCOOCH_3^{(l)} + H_2O^{(l)} \rightarrow HCOOH^{(l)} + CH_3OH^{(l)} \quad (9)$$

$$CH_4^{(g)} + \left(\frac{3-\Lambda}{2}\right)O_2^{(g)} + (\Lambda-1)H_2O^{(g)} \rightarrow HCOOH^{(l)} + (\Lambda)H_2^{(g)} \quad (3)$$

Carrying out a thermodynamic analysis of energetic self-sufficiency for the aforementioned process requires evaluation of the inlet and outlet streams' specific mass enthalpies and Gibbs free energies. To this end, all streams are considered to be pure, except for the air feed stream which is considered as an ideal gas mixture. All streams are also considered to be ideal gases, to enter and leave the system at $T_0 = 298.15\ K$ and $P_0 = 1\ \ bar$. The only exception is hydrogen, which is delivered at $P = 354.6\ \ bar$, which is a typical storage pressure for hydrogen-fueled vehicles. The necessary conditions for energetic self-sufficiency are then calculated using eqn. (4) below.

$$\left\{\begin{array}{c}\Delta\dot{H}_s(T_0) \triangleq \sum_{i\in\ S_I} H_i\dot{m}_i - \sum_{i\in\ S_O} H_i\dot{m}_i \geq 0 \\ \Delta\dot{G}_s(T_0) \triangleq \sum_{i\in S_I} G_i\dot{m}_i - \sum_{i\in S_O} G_i\dot{m}_i = \sum_{i\in\ S_I}(H_i - T_0{\cdot}S_i)\dot{m}_i \\ - \sum_{i\in\ S_O}(H_i - T_0{\cdot}S_i)\dot{m}_i \geq 0\end{array}\right\} \quad (4)$$

The dependence of these two conditions on the aforementioned parameter Λ is shown in Fig. 1.

As can be seen from Fig. 1, the formic acid – hydrogen co-production system can only be energetically self-sufficient if Λ is less than or equal to 2.23. Of course, this is only a necessary condition and the creation of an energetically self-sufficient flowsheet realizing reaction (3) may impose more stringent requirements on Λ.

No known process exists for the co-production of hydrogen and formic acid in a single step, as suggested by overall reaction (3). Nevertheless, its realization can be pursued through a suitable reaction cluster (also often referred to as thermochemical cycle, or Solvay cluster), whose individual steps are thermodynamically feasible (Andress et al., 2009; Holiastos and Manousiouthakis, 1998; Andress and Martin, 2010; Rudd et al., 1973; May and Rudd, 1976; Rotstein et al., 1982). Such a reaction cluster, employing commercially available technologies such as combustion (5), dry reforming (6), water-gas shift (7), and formic acid production via methyl formate formation (8) and subsequent hydrolysis (9), is shown in Fig. 2.

$$\left(\frac{3-\Lambda}{4}\right)[CH_4^{(g)} + 2O_2^{(g)} \rightarrow CO_2^{(g)} + 2H_2O^{(g)}] \quad (5)$$

$$\left(\frac{\Lambda+1}{4}\right)[CH_4^{(g)} + CO_2^{(g)} \rightarrow 2CO^{(g)} + 2H_2^{(g)}] \quad (6)$$

$$\left(\frac{\Lambda-1}{2}\right)[CO^{(g)} + H_2O^{(g)} \rightarrow CO_2^{(g)} + H_2^{(g)}] \quad (7)$$

$$CO^{(g)} + CH_3OH^{(l)} \rightarrow HCOOCH_3^{(l)} \quad (8)$$

$$HCOOCH_3^{(l)} + H_2O^{(l)} \rightarrow HCOOH^{(l)} + CH_3OH^{(l)} \quad (9)$$

Fig. 2. Reaction cluster for hydrogen and formic acid co-production.

$$CH_4^{(g)} + \left(\frac{3-\Lambda}{2}\right)O_2^{(g)} + (\Lambda-1)H_2O^{(g)} \rightarrow HCOOH^{(l)} + (\Lambda)H_2^{(g)}$$

A preliminary assessment of the external heating need of this cluster can be obtained through a 2nd law based thermodynamic analysis based on pinch inequalities (Holiastos and Manousiouthakis, 2002; Linnhoff and Hindmarsh, 1983; Linnhoff, 1993). This analysis can provide approximate estimates for the range of the parameter Λ leading to heating self-sufficiency. These estimates are not only based on the overall reaction and associated system inputs and outputs, but also account for the reaction cluster realizing the overall reaction, and the associated operating temperatures for each cluster reaction. These estimates can be obtained prior to the construction of a detailed process flowsheet realizing the proposed cluster, by considering that sensible heat effects can be ignored (as they can be approximately met through appropriate heat integration), reactions are carried out to completion, and product separation is largely attained through work and not heat consumption.

The approximate pinch analysis is carried out for the cluster using a minimum approach temperature $\Delta T_{\min} = 5\ K$. Parameterized by Λ, and starting from the reaction with the highest temperature (combustion at 1273 K), heat balances are carried out to ensure that heat is either utilized at the temperature that it is available at, or is cascaded downward from a high temperature to a lower temperature. Thus, net heat availability is assessed at every reaction operating temperature and pressure level, namely combustion reaction (P = 1 bar, T = 1273 K, exothermic), dry reforming reaction (P = 1 bar, T = 1073 K, endothermic), water-gas shift (WGS) two stage reactions (P = 21.3 bar (both), T = 623 K and T = 423 K, both exothermic), methyl formate synthesis (P = 170 bar, T = 353 K, exothermic), and formic acid synthesis (P = 9 bar, T = 393 K, exothermic). The WGS reaction heat load is considered to be available at T = 623 K since only small amounts of CO are converted to CO_2 in the low temperature WGS

Table 1
Cluster reaction operating conditions and heat loads.

S/N	Cluster reactions	Pressure (bar)	Temperature (K)	$\Delta H\,(kJ/mol)$	Notes
1	Combustion	1	1273	- 802.8	1
2	Dry Reforming	1	1073	+260.7	1
3	Water Gas Shift	21.3	623	−38.45	1
4	Methyl formate synthesis	170	353	−29.51	2
5	Formic acid synthesis	9	393	- 1.889	2

Notes
1. Values calculated via UNISIM using the Peng-Robinson equation of state.
2. Values calculated via UNISIM using the van Laar liquid activity coefficient model with the Kabadi Danner model for the vapor phase.

process. The heat loads for each reaction are calculated using UNISIM at their respective reaction temperatures and are listed in Table 1.

The aforementioned approximate pinch analysis then yields the following optimization problem:

$$\left\{\begin{array}{l} \nu(\Lambda) \triangleq \min\limits_{Q_{HU},Q_{CU}} Q_{HU} \\ s.\ t. \\ Q_{HU} \geq 0 \\ Q_{HU} + \ 0.25(3-\Lambda)|\Delta H_1| \geq 0 \\ Q_{HU} + \ 0.25(3-\Lambda)|\Delta H_1| - 0.25(1+\Lambda)|\Delta H_2| \geq 0 \\ Q_{HU} + \ 0.25(3-\Lambda)|\Delta H_1| - 0.25(1+\Lambda)|\Delta H_2| + 0.5(\Lambda-1)|\Delta H_3| \geq 0 \\ Q_{HU} + \ 0.25(3-\Lambda)|\Delta H_1| - 0.25(1+\Lambda)|\Delta H_2| + 0.5(\Lambda-1)|\Delta H_3| \\ \qquad + |\Delta H_4| \geq 0 \\ Q_{HU} + \ 0.25(3-\Lambda)|\Delta H_1| - 0.25(1+\Lambda)|\Delta H_2| + 0.5(\Lambda-1)|\Delta H_3| \\ \qquad\qquad + |\Delta H_4| + |\Delta H_5| \geq 0 \\ Q_{HU} + \ 0.25(3-\Lambda)|\Delta H_1| - 0.25(1+\Lambda)|\Delta H_2| + 0.5(\Lambda-1)|\Delta H_3| \\ \qquad\qquad + |\Delta H_4| + |\Delta H_5| = Q_{CU} \geq 0 \end{array}\right\} \tag{10}$$

Close examination of the structure of the above optimization problem's inequalities suggests that the second, fifth, sixth and seventh inequalities can be ignored without affecting optimality. (10) is then equivalent to:

$$\left\{\begin{array}{l} \nu(\Lambda) \triangleq \min\limits_{Q_{HU}} Q_{HU} \\ s.\ t. \\ Q_{HU} \geq 0 \\ Q_{HU} + \ 0.25(3-\Lambda)|\Delta H_1| - 0.25(1+\Lambda)|\Delta H_2| \geq 0 \\ Q_{HU} + \ 0.25(3-\Lambda)|\Delta H_1| - 0.25(1+\Lambda)|\Delta H_2| + 0.5(\Lambda-1)|\Delta H_3| \geq 0 \end{array}\right\} \tag{11}$$

The solution to equation (11) is derived analytically by evaluating various cases. To this end, the following quantities are evaluated using the heat of reaction values from Table 1:

$$\frac{3|\Delta H_1| - |\Delta H_2|}{|\Delta H_1| + |\Delta H_2|} = 2.02\ ; \quad \frac{3|\Delta H_1| - |\Delta H_2| - 2|\Delta H_3|}{|\Delta H_1| + |\Delta H_2| - 2|\Delta H_3|} = 2.10.$$

Case 1: $0 \leq \Lambda \leq 1$; It then holds $0 \leq \Lambda \leq 1 \leq \frac{3|\Delta H_1| - |\Delta H_2| - 2|\Delta H_3|}{|\Delta H_1| + |\Delta H_2| - 2|\Delta H_3|} = 2.10$, which in turn implies $0.25(3-\Lambda)|\Delta H_1| - 0.25(1+\Lambda)|\Delta H_2| \geq 0.25(3-\Lambda)|\Delta H_1| - 0.25(1+\Lambda)|\Delta H_2| + 0.5(\Lambda-1)|\Delta H_3| \geq 0$. Then $\{\nu(\Lambda) = 0\}$

Case 2: $1 \leq \Lambda \leq \frac{3|\Delta H_1| - |\Delta H_2|}{|\Delta H_1| + |\Delta H_2|} = 2.02$; This implies $0.25(3-\Lambda)|\Delta H_1| - 0.25(1+\Lambda)|\Delta H_2| + 0.5(\Lambda-1)|\Delta H_3|$. Then $\{\nu(\Lambda) = 0\}$

$\geq 0.25(3-\Lambda)|\Delta H_1| - 0.25(1+\Lambda)|\Delta H_2| \geq 0$

Case 3: $\frac{3|\Delta H_1| - |\Delta H_2|}{|\Delta H_1| + |\Delta H_2|} = 2.02 \leq \Lambda \leq \frac{3|\Delta H_1| - |\Delta H_2| - 2|\Delta H_3|}{|\Delta H_1| + |\Delta H_2| - 2|\Delta H_3|} = 2.10 \leq 3$; This implies

$0.25(3-\Lambda)|\Delta H_1| - 0.25(1+\Lambda)|\Delta H_2| + 0.5(\Lambda-1)|\Delta H_3| \geq 0.25(3-\Lambda)|\Delta H_1| - 0.25(1+\Lambda)|\Delta H_2|$

Then $\{\nu(\Lambda) = 0.25[\Lambda(|\Delta H_1| + |\Delta H_2|) - (3|\Delta H_1| - |\Delta H_2|)]\}$

Case 4: $\frac{3|\Delta H_1| - |\Delta H_2|}{|\Delta H_1| + |\Delta H_2|} = 2.02 \leq \frac{3|\Delta H_1| - |\Delta H_2| - 2|\Delta H_3|}{|\Delta H_1| + |\Delta H_2| - 2|\Delta H_3|} = 2.10 \leq \Lambda \leq 3$; This implies $0 \geq 0.25(3-\Lambda)|\Delta H_1| - 0.25(1+\Lambda)|\Delta H_2| + 0.5(\Lambda-1)|\Delta H_3|$.

$\geq 0.25(3-\Lambda)|\Delta H_1| - 0.25(1+\Lambda)|\Delta H_2|$

Then $\{\nu(\Lambda) = 0.25[\Lambda(|\Delta H_1| + |\Delta H_2|) - (3|\Delta H_1| - |\Delta H_2|)]\}$

In summary,

$$\nu(\Lambda) = \left\{\begin{array}{l} 0; \qquad 0 \leq \Lambda \leq \frac{3|\Delta H_1| - |\Delta H_2|}{|\Delta H_1| + |\Delta H_2|} = 2.02 \\ 0.25[\Lambda(|\Delta H_1| + |\Delta H_2|) - (3|\Delta H_1| - |\Delta H_2|)]; \\ \frac{3|\Delta H_1| - |\Delta H_2|}{|\Delta H_1| + |\Delta H_2|} = 2.02 \leq \Lambda \leq 3 \end{array}\right\} \tag{12}$$

Equation (12) above suggests that, based on the outlined approximate pinch analysis, the hydrogen and formic acid co-production process can only be energetically self-sufficient, if the molar ratio Λ of hydrogen produced to methane feed is greater than 0 and less than 2.02, i.e. $0 \leq \Lambda \leq 2.02$. Thus, the approximate pinch analysis of the reaction cluster proposed for the realization of the overall reaction reduces the upper limit of Λ from 2.23 to 2.02. This is because it takes into account the operating temperatures and associated heat loads of the cluster's constitutive reactions, while the earlier upper bound was obtained based only on the inlet-outlet thermodynamic properties of the overall system.

3. A realization of the proposed hydrogen-formic acid production method

Next, a process flowsheet is described that realizes the proposed reaction cluster using commercially available processes. This overall hydrogen-formic acid co-production process can be partitioned into six subsystems:

1. Combustion subsystem: This system contains an air separation PSA system, a burner and a water separator.
2. Dry reforming subsystem: This contains the preheating devices and the dry reforming reactor.
3. H_2/CO PSA subsystem: This subsystem processes the stream coming from the dry reforming reactor, through a dehumidifier, hydrogen PSA, carbon monoxide PSA and three pressurization systems. Carbon monoxide is purified and pressurized for its use downstream, while hydrogen is purified and pressurized for its final delivery.
4. Water-gas shift subsystem: This subsystem contains the water-gas shift reactor which utilizes fresh water and carbon monoxide from the H_2/CO PSA subsystem to produce hydrogen and carbon dioxide.
5. Methyl formate subsystem: This subsystem comprises the methyl formate reactor and dual pressure methyl formate/methanol purifier.
6. Formic acid subsystem: This subsystem contains the formic acid reactor, double azeotrope separator, excess water separator and dual pressure formic acid purifier.

A schematic of the overall process is shown in Fig. 3.

3.1. Combustion subsystem

Pure oxygen for the combustion subsystem is separated from air via the system described in (Pena Lopez and Manousiouthakis, 2011). Air enters a two-stage PSA unit at atmospheric conditions (P = 1 bar, T = 298 K) and pure oxygen exits at the same conditions. The removal of nitrogen is accomplished in the first stage via a zeolite packed PSA unit and argon in the second stage via a carbon molecular sieve (CMS) adsorbent (Armond et al., 1980; Richter et al., 1986; Santos et al., 2007; Hayashi et al., 1996; Jee et al., 2005; Ruthven et al., 1994; Vansant and Dewolfs, 1989). The air-PSA unit consumes 48,000 kJ per kmol of oxygen produced (Ruthven et al., 1994). This work requirement is accounted for in the heat and power integration analysis that follows.

Purified oxygen at 1 bar, 298 K is mixed with fresh methane, recycled water, waste from the H_2/CO PSA and a recycle stream from the formic acid and methyl formate subsystems. The mixture, which contains 11% steam as diluent, is heated to 1223 K and fed into the combustion reactor which operates at 1273 K and 1 bar. The combustor effluent is a high quality hot stream that contributes to the satisfaction of the flowsheet's energetic needs (e.g. satisfaction of the reformer's endothermic load). The combustor exit stream is partially condensed and distilled via a flash separator to separate the carbon dioxide and water. The water stream is partially recycled to the entrance of the reactor, while the rest is directed to the formic acid subsystem. The carbon dioxide-rich stream is directed to the dry reforming subsystem.

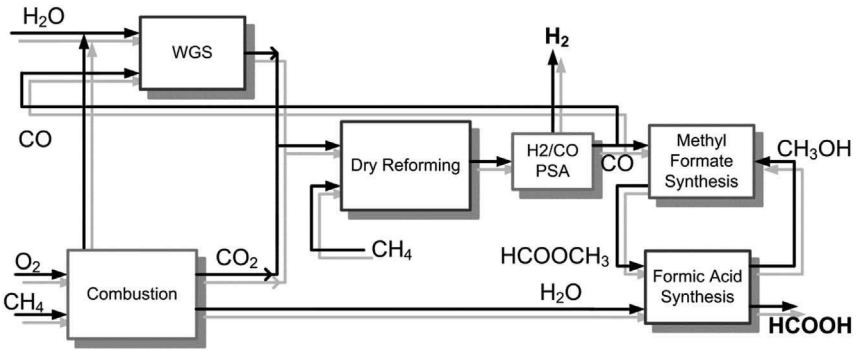

Fig. 3. Process flowsheet realizing proposed reaction cluster.

3.2. Dry reforming subsystem

The dry reforming reaction is a highly endothermic reaction that produces syngas (H_2/CO) from methane and carbon dioxide (Eqn. (13)), as shown below.

$$CH_4^{(g)} + CO_2^{(g)} \rightleftharpoons 2CO^{(g)} + 2H_2^{(g)} \quad (13)$$

It is typically carried out, using Ni/Ce-based catalysts, at temperatures ranging from 873 to 1273 K (Verykios, 2003; Guo et al., 2004; Laosiripojana and Assabumrungrat, 2005). In this work, the reactor is operated at 1073 K and 1 bar to achieve high conversion. As a result, its operation creates a large, high temperature, endothermic heat load for the overall process flowsheet, which represents a significant contribution to the overall system's hot utility use. The dry reformer's feed is the vapor product of a flash separator, whose feed is a mixture of recycled carbon dioxide-rich streams and natural gas, and liquid product is water that is sent to the combustion subsystem to form part of the diluent for the combustion reactor. The resulting dry reformer feed possesses a CH_4/CO_2 molar ratio equal to 1.1. At the given conditions, the equilibrium conversion of carbon dioxide in the dry reformer is 96.6%, generating a stream containing primarily hydrogen and carbon monoxide and some carbon dioxide, methane and water, that is directed to the H_2/CO PSA.

3.3. H_2/CO PSA subsystem

The structure of the H_2 and CO separation subsystem is largely based on (Krishnamurthy, 1992). The exit of the dry reformer is passed through a dryer operating at room temperature, and containing desiccant material such as alumina, silica or zeolite. The dryer removes 99.99% of the water contained in its feed, and its dried H_2/CO-rich stream exit is pressurized through 4 equal-ratio compressors to 20 atm. The compressed mixture is then passed through a H_2 PSA, which delivers 80% of its fed hydrogen as a pure product, at 99.999+ % purity, and 20 atm. This pure hydrogen product is subsequently further compressed to a delivery pressure of 354.6 bar through a 4-compressor pressure train. The H_2 PSA's adsorbent material typically consists of molecular carbon sieve/activated carbon or 5A zeolite sieves, and exhibits greater affinity for carbon dioxide, methane and carbon monoxide than for hydrogen. Once the H_2 PSA's bed is deemed to be near saturation, it is depressurized, until reaching a pressure of 1.7 bar, thus resulting into a carbon monoxide-rich stream that is sent to the carbon monoxide PSA. The H_2 PSA continues to be depressurized until atmospheric pressure, and it is the purged with hydrogen to generate a waste gas purge stream, which is mixed with a waste gas stream from the CO PSA. This mixture is recycled to the dry reformer subsystem. The carbon monoxide-rich stream is pressurized up to 3 bar, and is then passed through a CO PSA containing an adsorbent having greater affinity for carbon monoxide than for hydrogen, carbon dioxide and methane. Such suitable adsorption materials are copper exchanged substrates (copper exchanged Y-type aluminosilicate zeolite molecular sieves, copper exchanged alumina, copper exchanged activated carbon, and their combinations). The non-adsorbed stream is compressed and mixed with the waste gas of the H_2 PSA. During its desorption phase, the CO PSA unit is depressurized to 1 bar to withdraw a high purity CO stream that is compressed, via a 4-compressor train, to 21.3 bar (equal to the operating pressure of the water-gas shift reactor) and directed to the water-gas shift subsystem. The remaining carbon monoxide is further pressurized to 170 bar (the operating pressure of the methyl formate reactor) and sent to the methyl formate subsystem.

3.4. Water-gas shift subsystem

The reaction cluster employed for the realization of the overall reaction, utilizes the water-gas shift (WGS) reaction shown below (Eqn. (14)), to increase the overall system's hydrogen production, and thus complement the hydrogen produced by the dry reforming process.

$$CO^{(g)} + H_2O^{(g)} \rightleftharpoons CO_2^{(g)} + H_2^{(g)} \quad (14)$$

This reaction is typically carried out under catalytic conditions and the materials are Ni-, Cu-, Au- and Zn-based (Li et al., 2000; Andreeva et al., 2002). For industrial applications such as the production of ammonia, the water-gas shift reaction is carried out in two separate stages with two types of catalysts. One is a high-temperature (573–773 K) shift catalyst based on iron oxide promoted with chromium oxide, while the other is a low-temperature (423–573 K) shift catalyst composed of copper, zinc oxide and alumina (Li et al., 2000; Rhodes et al., 1995).

The water-gas shift subsystem utilizes fresh feed water and carbon monoxide produced from the dry reforming subsystem and purified in the CO PSA. The mixture is heated to 623 K and fed to the high-temperature WGS reactor. The exit is cooled to 423 K and fed to the low-temperature WGS reactor. The exit, consisting primarily of carbon dioxide and hydrogen, is depressurized to 1 bar and sent to the dry reformer subsystem.

3.5. Methyl formate subsystem

Methyl formate is produced via carbonylation of liquid methanol with carbon monoxide, in the presence of a basic catalyst, as shown below (Eqn. (15)).

$$CO^{(g)} + CH_3OH^{(l)} \rightleftharpoons HCOOCH_3^{(l)} \quad (15)$$

The carbon monoxide is received from the H_2/CO PSA at 170 bar, mixed with streams containing unreacted methanol and methanol recovered from the formic acid subsystem, heated to 353 K, and fed to the methyl formate reactor. This reaction was first described by BASF in 1925 (Reutemann and Kieczka, 2000). The reaction (Eqn. (15)) is favored at high pressures and low temperatures. The catalysts proposed for this process include sodium methoxide and potassium methoxide. High reaction conversion occurs at operating pressures ranging from 10 bar to 170 bar. The exit of the reactor, consisting of unreacted

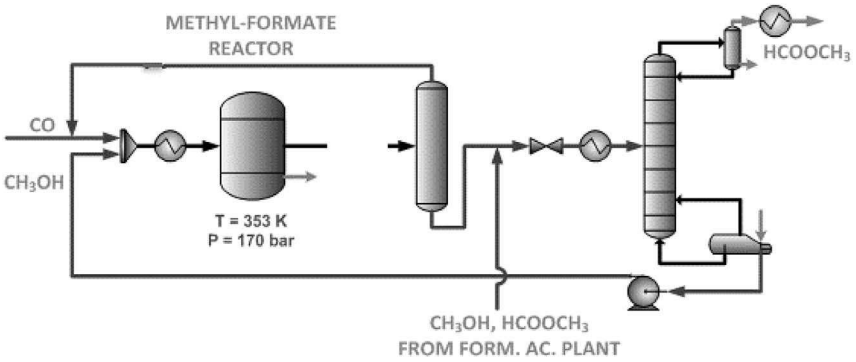

Fig. 4. Methyl formate subsystem.

carbon monoxide, methyl formate and methanol, is fed to a flash separator, whose gaseous product is recycled to the methyl formate reactor, while its liquid product is mixed with a methyl formate/methanol azeotropic stream being recycled from the formic acid subsystem. The resulting mixture is depressurized to 0.5 bar, heated up to 307 K and fed to a distillation column, whose bottom product is a methanol-rich stream at 320 K, while its top product is pure methyl formate (99%) at 287 K. The bottom methanol-rich stream is recycled to the methyl formate reactor, while the top pure methyl formate stream is sent to the formic acid subsystem. The methyl formate subsystem is shown in Fig. 4 below.

3.6. Formic acid subsystem

Formic acid is produced via autocatalytic hydrolysis of methyl formate (Eqn. (16)), as shown below.

$$HCOOCH_3^{(l)} + H_2O^{(l)} \rightleftharpoons CH_3OH^{(l)} + HCOOH^{(l)} \quad (16)$$

This subsystem's methyl formate feed is received from the formate generation subsystem, while its water feed consists of fresh and recycled water. The operating conditions were chosen to match the Kemira-Leonard Process (393 K and 9 bar) (Reutemann and Kieczka, 2000). The inherent equilibrium conversion limitations of (16) require the use of a large excess of either methyl formate or water. The latter option is employed, and a water to methyl formate ratio of 5–6 has been found to be suitable. The thermodynamic behavior of mixtures containing the reactants and products of (Eqn. (16)), includes the existence of two binary azeotropes: methyl formate/methanol and water/formic acid. Nevertheless, the composition of the mixture exiting the Kemira-Leonard reactor is such that a separation system can be devised that delivers pure formic acid as a product, and additional streams that can be recycled to other subsystems of the overall flowsheet.

The high purity methyl formate, from the methyl formate subsystem, is pressurized to 9 bar and mixed with fresh water and recycled water from the combustion subsystem. The resulting mixture, featuring a water to methyl formate ratio of 5.1 as suggested in the literature (Reutemann and Kieczka, 2000), is heated to 393 K and fed to the formic acid reactor. This reactor's exit is depressurized to 1 bar, cooled down, and fed to a distillation column, whose top product is a methanol-methyl formate azeotropic mixture at 317 K, while its bottom product is an aqueous mixture at 373 K. The top product is recycled to the methyl formate subsystem as mentioned above, while the bottom product is sent to a water recovery column, where pure water is removed as a top product at 373 K, while the bottom product is a formic acid (55% molar) - water mixture that is fed to a dual-pressure distillation sequence for formic acid purification.

The aforementioned formic acid-water bottom product is mixed with a formic acid-water azeotropic mixture, emanating from the bottom of the low-pressure column of the dual pressure distillation system. The resulting stream is pressurized to 12 bar, and fed to the first, high pressure, distillation column of the dual pressure distillation system. This column's top product is a water-rich stream at 458 K that is recycled to the water recovery column, while the column's bottom product is a formic acid-water azeotropic mixture at 482 K, that is throttled to 0.5 bar. This stream is mixed with a portion of the final product pure formic acid stream, so as to move the resulting stream's formic acid content above the low-pressure azeotropic composition. This stream is then fed to the low-pressure column of the dual pressure distillation system, where it is separated into a top pure formic acid product (99%), and a bottom product that is fed to the high-pressure column, as stated above. The formic acid subsystem is shown in Fig. 5 below.

4. Simulation and heat/power integration of proposed process realization

The aforementioned subsystems are composed into an overall process flowsheet, which is presented in Fig. 6. The flowsheet takes as

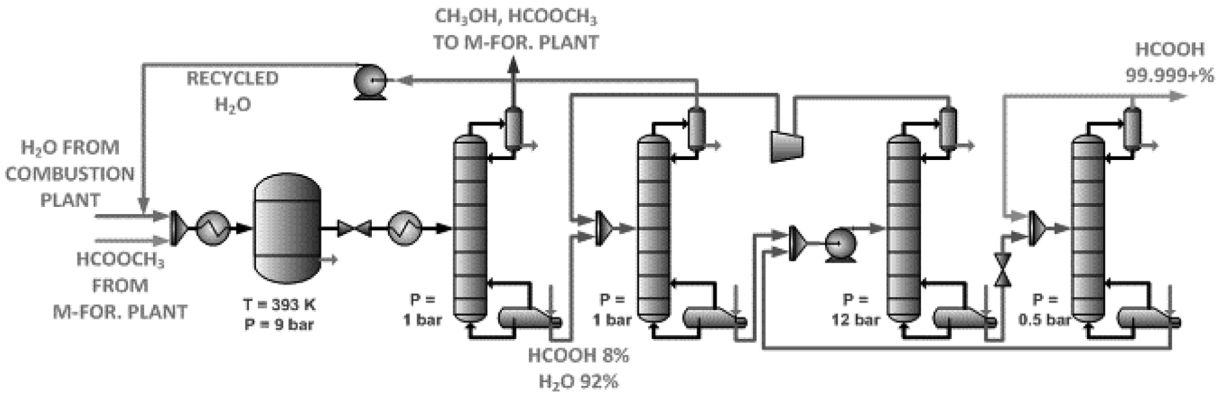

Fig. 5. Formic acid subsystem.

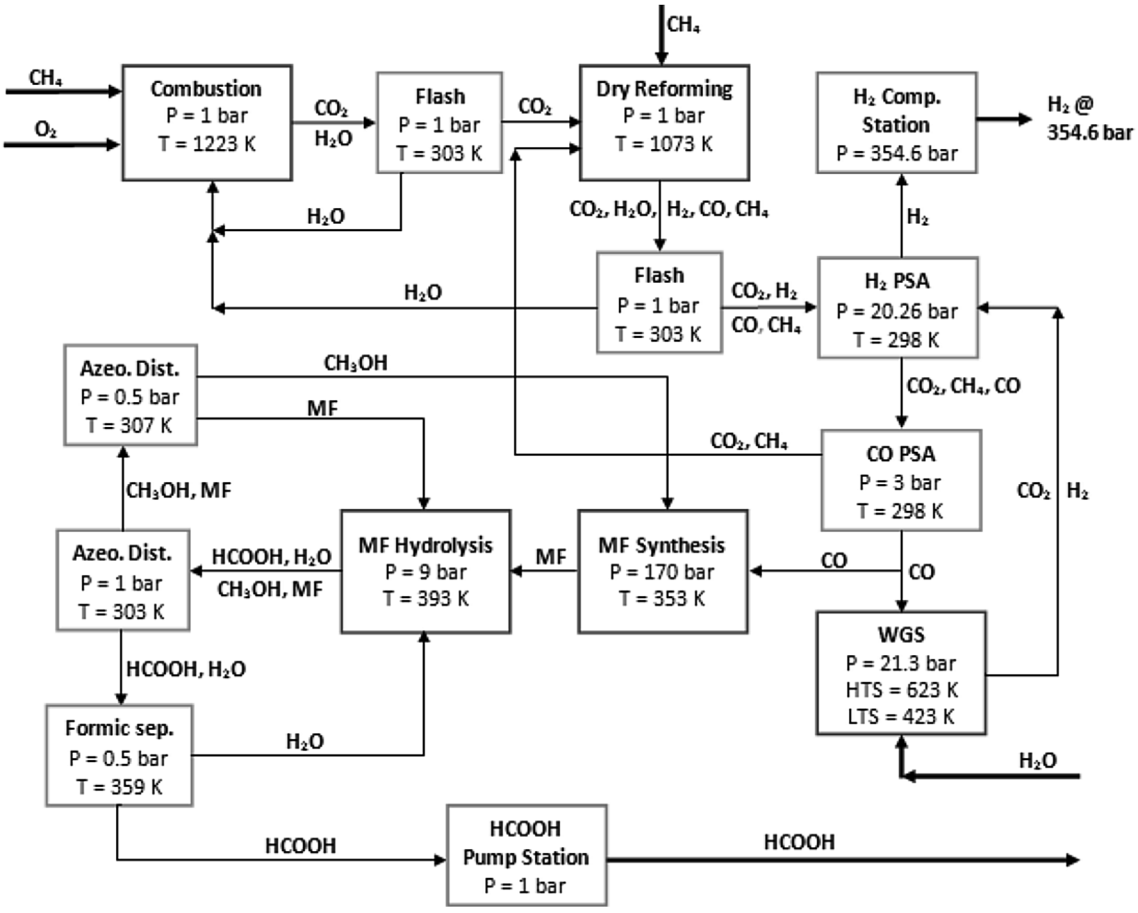

Fig. 6. Overall process simulation in UniSim® design.

material inputs, natural gas (methane), water and oxygen at 1 bar and 298 K, and produces hydrogen at 354.6 bar and 298 K and high purity formic acid (99.9%) at 1 bar and 298 K. The proposed process flowsheet is simulated using the software UniSim Design®. The flowsheet's energetic behavior is assessed through heat and power integration analysis, carried out using UCLA in-house software. This analysis implements the theory set forth in Ref. (Posada and Manousiouthakis, 2005; Holiastos and Manousiouthakis, 2002)., and identifies the flowsheet's minimum hot/cold/electric utility cost. To ensure energetic self-sufficiency, only cold utilities are allowed. Heat engines and heat pumps are also utilized in the analysis. Cold utility is available at 298 K and the work/cold utility cost ratio is 25 to 2, with the minimum approach temperature fixed at 5 K (Pena Lopez and Manousiouthakis, 2011).

The necessary conditions for energetic self-sufficiency, and the approximate pinch analysis presented earlier, suggest respectively that $\Lambda \leq 2.23$, and $\Lambda \leq 2.02$ for the overall process to be energetically self-sufficient. However, depending on the particulars of any particular realizing flowsheet, the rate of entropy generation may vary from design to design, depending on the value of Λ. Thus, first an overall process design is chosen corresponding to $\Lambda = 2$. Carrying out the aforementioned heat and power integration analysis, suggests that this design is not energetically self-sufficient. This process is repeated for decreasing values of Λ, until the subsequent heat and power integration analysis identifies the flowsheet to be self-sufficient. This turns out to be the case for $\Lambda = 1.03$, which results into the flowsheet presented in Fig. 6. This flowsheet maximizes hydrogen production, while being energetically self-sufficient.

The simulation of the identified flowsheet employs the Peng-Robinson-Stryjek-Vera equation of state for all subsystems, except for the formic acid plant in which the van Laar liquid activity coefficient model coupled with the Kabadi-Danner model for the vapor phase is utilized (Honeywell, 2008). The van Laar, Kabadi-Danner model combination captures to a large extent the methyl formate/methanol and water/formic acid azeotropic vapor-liquid equilibrium behavior. The dry reformer and combustor are represented by Gibbs free energy minimization reactors and the water-gas shift, methyl formate, and formic acid reactors are represented as equilibrium reactors for the corresponding reaction. No pressure losses are considered for the heat exchange devices (heaters and coolers), while the compressors work at 75% adiabatic efficiency.

The natural gas entering the flowsheet services both the dry reforming and combustion subsystems with the split ratio defined in terms of the molar ratio Λ of hydrogen produced to natural gas fed. When Λ increases, the natural gas flow to the dry reforming subsystem increases, while a lower value of Λ generates more energy, by increasing the amount of methane flowing through the combustion subsystem.

5. Results and discussion

Several iterations were carried out to determine the maximum Λ hydrogen/methane molar ratio for which the overall flowsheet is energetically self-sufficient. As starting point for these iterations, a flowsheet was employed corresponding to $\Lambda = 2.02$, as identified by the aforementioned approximate pinch analysis. The detailed heat and power integration analysis, with no hot utility available, indicates that this flowsheet is not energetically self-sufficient due to work consumption. This procedure is repeated for lower values of Λ until the total work (work generated from heat and power integration plus work demand of the flowsheet) is less than or equal to zero. This evolutionary

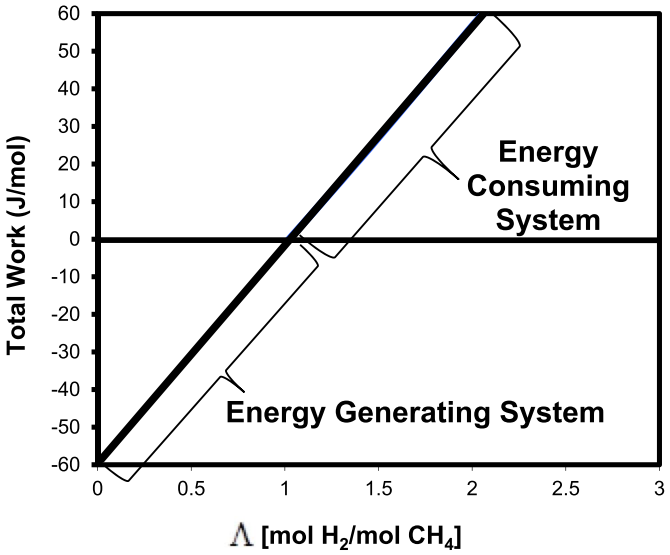

Fig. 7. Total Work dependence on Λ.

process is captured in Fig. 7, where the flowsheet's total work consumption ($W \geq 0$) is plotted as a function of Λ. This suggests that the above process becomes energetically self-sufficient for values of $\Lambda \leq 1.03$.

The temperature-entropy change diagram generated by the heat and power integration analysis for the $\Lambda = 1.03$ design is shown in Fig. 8a. It indicates that the flowsheet requires the operation of two heat engines and two heat pumps to satisfy its energy requirements. The hot and cold composite curves on the temperature-entropy diagram intersect each other at 300 K, 333 K and 485 K delineating the heat engine and heat pump operating regions. The flowsheet's overall enthalpy balance is presented in the temperature-enthalpy diagram shown in Fig. 8b, which also illustrates the work generated by the heat exchange/engine/pump network, which is then used to meet the work needs of the flowsheet's work consuming operations.

To establish the superior economic potential of this flowsheet, a brief rudimentary operating cost analysis is carried out for the energetically self-sufficient $\Lambda = 1.03$ design and the energetically deficient $\Lambda = 2.02$ design. The economic potential of both cases is assessed by examining its raw material cost and saleable product revenue. The raw material related operating costs of both flow-sheets consist mainly of natural gas at 5.23 $/(10ft)^3 (Energy Information Administration, 2011) (i.e. 0.282 $/kg of CH_4), electricity consumption for oxygen separation at 0.105 $/kWh (Rath, 2010), and water at 0.000285 $/kg (Rath, 2010), while the revenue obtained by the plant's two main products is 0.70 $/kg formic acid (ICIS, 2003; ICIS, 2006), and 3.64 $/kg hydrogen (Energy Information Administration, 2011). The power consumption for oxygen production is based on the air-PSA value of

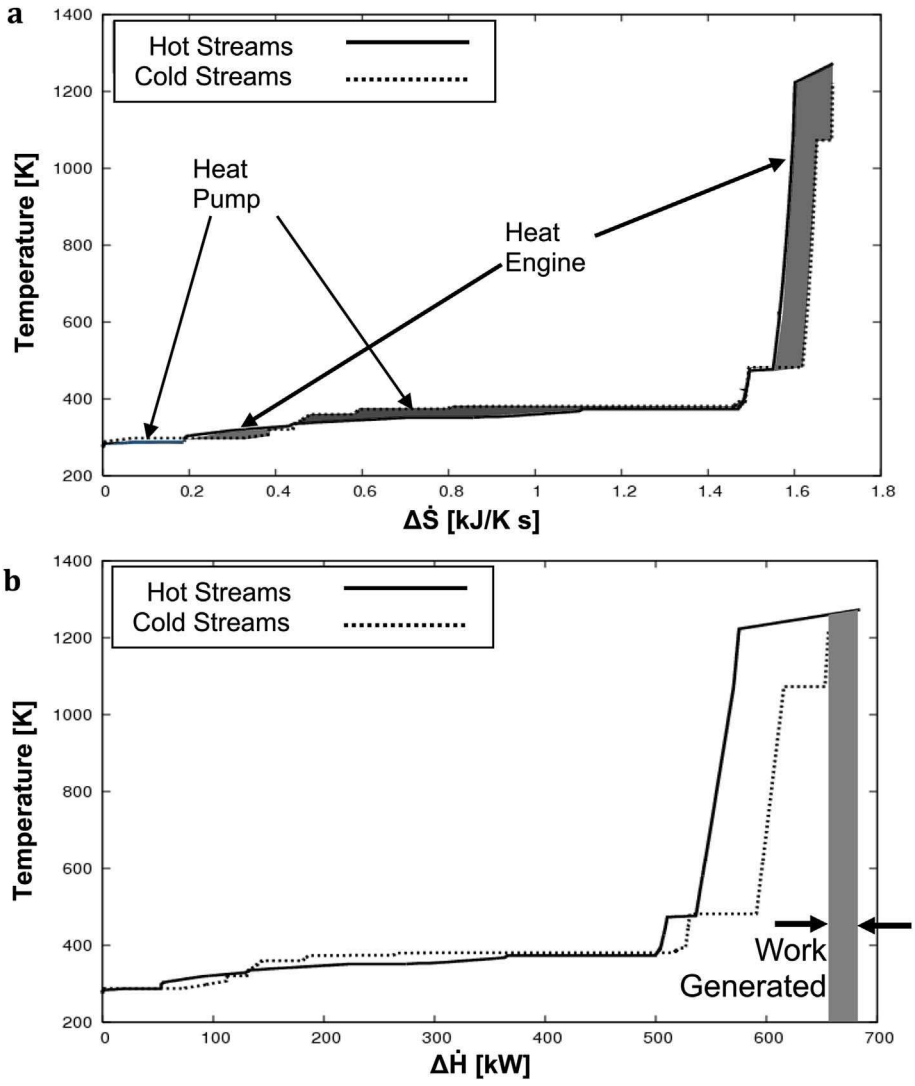

Fig. 8. (8a) Temperature-Entropy Change Diagram for $\Lambda = 1.03$ Design; (8b) Temperature-Enthalpy Change Diagram for $\Lambda = 1.03$ Design.

Table 2a
Operating cost analysis of process co-producing formic acid and hydrogen at an energetically self-sufficient hydrogen/methane molar ratio of 1.03.

	Unit Cost	Unit	Unit Cost Ref.	Net Amount Consumed	Unit	Total	Unit
Expenditure							
Natural Gas	0.282	($/kg)	(Energy Information Administration, 2011)	16.043	kg/h	4.524	($/h)
O_2 Production Power Consumption	0.105	($/kWh)	(Rath, 2010)	13.134	kW	1.379	($/h)
Water	0.000285	($/kg)	(Rath, 2010)	0.541	kg/h	0.00015	($/h)
Total Expenditure:						**5.903**	**($/h)**
Revenue							
Formic acid	0.70	($/kg)	(ICIS, 2003; ICIS, 2006)	46.030	kg/h	32.221	($/h)
Hydrogen	3.64	($/kg)	(Energy Information Administration, 2011)	2.076	kg/h	7.557	($/h)
Total Revenue:						**39.778**	**($/h)**
Profit Margin:						**33.875**	**($/h)**

Table 2b
Operating cost analysis of process co-producing formic acid and hydrogen at an energetically deficient hydrogen/methane molar ratio of 2.02.

	Unit Cost	Unit	Unit Cost Ref.	Net Amount Consumed	Unit	Total	Unit
Expenditure							
Natural Gas	0.282	($/kg)	(Energy Information Administration, 2011)	16.043	kg/h	4.524	($/h)
O_2 Production Power Consumption	0.105	($/kWh)	(Rath, 2010)	6.534	kW	0.686	($/h)
Work requirement from surrounding	0.105	($/kWh)	(Rath, 2010)	0.0167	kW	0.00175	($/h)
Water	0.000285	($/kg)	(Rath, 2010)	18.380	kg/h	0.00524	($/h)
Total Expenditure:						**5.217**	**($/h)**
Revenue							
Formic acid	0.70	($/kg)	(ICIS, 2003; ICIS, 2006)	46.030	kg/h	32.221	($/h)
Hydrogen	3.64	($/kg)	(Energy Information Administration, 2011)	4.072	kg/h	14.822	($/h)
Total Revenue:						**47.043**	**($/h)**
Profit Margin:						**41.826**	**($/h)**

48,000 kJ per kmol of oxygen produced (Ruthven et al., 1994), while the work requirement for the energetically deficient case is calculated from Fig. 7 for the selected hydrogen/methane molar ratio, Λ. All other values are calculated based on the overall reaction of the co-production process.

As shown in Table 2a, for the energetically self-sufficient $\Lambda = 1.03$ design, a revenue of $32.221/h (or 7.12 times the natural gas cost) is obtained from formic acid sales alone (i.e. when hydrogen is given for free) and a revenue of $39.778/h (or 8.79 times the natural gas cost) is obtained from the sale of both formic acid and hydrogen.

Similarly in Table 2b, for the energetically deficient $\Lambda = 2.02$ design, a revenue of $32.221/h (or 7.12 times the natural gas cost) is obtained from formic acid sales alone (i.e. when hydrogen is given for free) and a revenue of $47.043/h (or 10.40 times the natural gas cost) is obtained from the sale of both formic acid and hydrogen. The net profit of the $\Lambda = 1.03$ and $\Lambda = 2.02$ designs is $33.875/h and $41.826/h respectively, representing a 23.47% increase as the process moves from being energetically self-sufficient at $\Lambda = 1.03$ to being energetically deficient at $\Lambda = 2.02$. The $\Lambda = 2.02$ design is largely profitable because only a small amount of work (0.0167 kW) is required from the surroundings to drive the process. However, as can be seen from both Tables 2a and 2b, both designs demonstrate economic attractiveness of the co-production process.

6. Conclusions

An energetically self-sufficient process for the production of hydrogen and formic acid from natural gas is developed. To accomplish this goal, an overall reaction for the process is first proposed, which is parametrized in terms of the molar ratio Λ of hydrogen produced to natural gas consumed. Subsequently, this overall reaction is realized by a reaction cluster employing commercially available reaction processes, such as natural gas combustion, dry reforming, water gas shift reaction, methyl formate synthesis, and subsequent hydrolysis to generate formic acid. The resulting reactive subsystems, are combined with separative subsystems that are also commercially available, such as pressure swing adsorption, distillation, and flash separation, to help form an overall process flowsheet. A detailed simulation of this overall flowsheet is then carried out, within the software environment UniSim Design® R443. Heat and power integration analysis of the overall process leads to the conclusion that energetic self-sufficiency can be ascertained for a process with maximum hydrogen production of 1.03 mol of H_2, and 1 mol of formic acid per mole of CH_4. This same heat and power integration analysis reveals the need for 2 heat engine and 2 heat pump subnetworks to make the flowsheet energetically self-sufficient. An operating cost analysis suggests a revenue value of 712% times the cost of natural gas, when only formic acid is sold (hydrogen is given off for free), and a revenue value of 878% times the cost of natural gas when hydrogen is sold alongside formic acid at commercial prices. These revenue values become 712% and 1040% times the cost of natural gas, if the process is operated at an energetically deficient hydrogen/methane molar ratio of 2.02. At this operating point, the net profit is 23.47% higher than that for the $\Lambda = 1.03$ design case. These returns do not include any carbon emission reduction credits associated with the fact that the process does not generate any carbon dioxide emissions.

Acknowledgements

Financial support through NSF grant 1650574 “EAGER Optimal Modular Process Synthesis” is gratefully acknowledged. Financial Support for Mr. Jorge A. Pena Lopez, through CONACYT Mexico, and for Mr. Ibubeleye Somiari, through a Presidential Special Scholarship scheme for Innovation and Development (PRESSID) from the National Universities Commission of Nigeria, is also gratefully acknowledged.

References

American Lung Association, 2007. State of Air. lungusa.org 2007 [cited; Available from: http://www.lungusa.org/assets/documents/publications/state-of-the-air/state-of-the-air-report-2007.pdf.

Andreeva, D., et al., 2002. Low-temperature water-gas shift reaction over Au/CeO2 catalysts. Catal. Today 72 (1–2), 51–57.

Andress, R.J., Martin, L.L., 2010. On the synthesis of hydrogen producing alternative

thermochemical cycles with electrochemical steps. Int. J. Hydrogen Energy 35 (3), 958–965.
Andress, R.J., et al., 2009. A systematic methodology for the evaluation of alternative thermochemical cycles for hydrogen production. Int. J. Hydrogen Energy 34 (9), 4146–4154.
Armond, J.W., Webber, D.A., Smith, K.C., 1980. Gas separation. US Patent 4,190,424.
Energy Information Administration, July 2011. Natural Gas Monthly.
Energy Information Administration, July 2011. Weekly U.S. Retail Gasoline Prices, Regular Grade.
Guo, J.J., et al., 2004. Dry reforming of methane over nickel catalysts supported on magnesium aluminate spinels. Appl. Catal. a-General 273 (1–2), 75–82.
Hayashi, S., Kawai, M., Kaneko, T., 1996. Dynamics of high purity oxygen PSA. Gas Sep. Purif. 10 (1), 19–23.
Holiastos, K., Manousiouthakis, V., 1998. Automatic synthesis of thermodynamically feasible reaction clusters. AIChE J. 44 (1), 164–173.
Holiastos, K., Manousiouthakis, V., 2002. Minimum hot/cold/electric utility cost for heat exchange networks. Comput. Chem. Eng. 26 (1), 3–16.
Honeywell, 2008. UniSim ® Thermo Reference Guide.
ICIS, July 2003. Chemical Business, Product Profile: Formic Acid.
ICIS, July 2006. Chemical Business, Chemical Profile: Formic Acid.
Jee, J.-G., Kim, M.-B., Lee, C.-H., 2005. Pressure swing adsorption processes to purify oxygen using a carbon molecular sieve. Chem. Eng. Sci. 60 (3), 869–882.
Krishnamurthy, R.P.,N.J., 1992. Hydrogen and carbon monoxide production by hydrocarbon steam reforming and pressure swing adsorption purification. The BOC Group, Inc. (Murray Hill, NJ), United States.
Laosiripojana, N., Assabumrungrat, S., 2005. Catalytic dry reforming of methane over high surface area ceria. Appl. Catal. B Environ. 60 (1–2), 107–116.
Li, K., Fu, Q., Flytzani-Slephanopoulos, M., 2000. Low-temperature water-gas shift reaction over Cu- and Ni-loaded cerium oxide catalysts. Appl. Catal. B-Environmental 27 (3), 179–191.
Linnhoff, B., 1993. Pinch analysis - a state-of-the-art overview. Chem. Eng. Res. Des. 71 (A5), 503–522.
Linnhoff, B., Hindmarsh, E., 1983. The pinch design method for heat exchanger networks. Chem. Eng. Sci. 38 (5), 745–763.
May, D., Rudd, D.F., 1976. Development of solvay clusters of chemical reactions. Chem. Eng. Sci. 31 (1), 59–69.
Pena Lopez, J., Manousiouthakis, V., 2011. Natural gas based hydrogen production with zero carbon dioxide emissions. Int. J. Hydrogen Energy 36, 12853–12868.
Pieter, T., 2017. Trends in Atmospheric Carbon Dioxide - Mauna Loa. esrl.noaa.Gov. [cited; Available from: https://www.esrl.noaa.gov/gmd/ccgg/trends/global.html.
Posada, A., Manousiouthakis, V., 2005. Heat and power integration of methane reforming based hydrogen production. Industrial Eng. Chem. Res. 44 (24), 9113–9119.
Posada, A., Manousiouthakis, V., 2006. Hydrogen and dry ice production through phase equilibrium separation and methane reforming. J. Power Sources 156 (2), 480–488.
Ramage, M.P., Agrawal, R., 2004. The Hydrogen Economy: Opportunities, Cost, Barriers, and R&D Needs. National Research Council of the National Academies.
Rath, L.K., 2010. Assessment of Hydrogen Production with CO_2 Capture Volume 1: Baseline State-of-the-art Plants. DoE/NETL, Report, vol. 1434.
Reutemann, W., Kieczka, H., 2000. Formic Acid, in Ullmann's Encyclopedia of Industrial Chemistry. Wiley-VCH Verlag GmbH & Co. KGaA.
Rhodes, C., Hutchings, G.J., Ward, A.M., 1995. Water-gas shift reaction: finding the mechanistic boundary. Catal. Today 23 (1), 43–58.
Richter, E., et al., 1986. Process and Apparatus for Producing Oxygen with a Low Proportion of Argon from Air. U.S. Patent 4,566,881.
Rotstein, E., Resasco, D., Stephanopoulos, G., 1982. Studies on the synthesis of chemical reaction paths—I: reaction characteristics in the (ΔG, T) space and a primitive synthesis procedure. Chem. Eng. Sci. 37 (9), 1337–1352.
Rudd, D.F., Powers, G.J., Siirola, J.J., 1973. Process Synthesis. Prentice-Hall, Englewood Cliffs, NJ.
Ruthven, D.M., Farooq, S., Knaebel, K.S., 1994. Pressure Swing Adsorption. VCH Publishers, New York, N.Y.
Santos, J.C., et al., 2007. High-purity oxygen production by pressure swing adsorption. Industrial Eng. Chem. Res. 46 (2), 591–599.
Scholz, W.H., 1993. Processes for industrial production of hydrogen and associated environmental effects. Gas Sep. Purif. 7 (3), 131–139.
Spath, P.L., Mann, M.K., 2001. Life Cycle Assessment of Hydrogen Production via Natural Gas Steam Reforming. National Renewable Energy Laboratory, Golden, CO.
Vansant, E.F., Dewolfs, R., 1989. In: Gas separation Technology: Proceedings of the International Symposium on Gas Separation Technology, Antwerp, Belgium, September 10-15. Elsevier, Amsterdam, Netherlands; New York.
Verykios, X.E., 2003. Catalytic dry reforming of natural gas for the production of chemicals and hydrogen. Int. J. Hydrogen Energy 28 (10), 1045–1063.